

Gamma cyclodextrin & Prontosil antibiotic as a bio interface structure for drug delivery systems: a UV sensor (via QM/MM)

Maryam Derakhshandeh¹, Majid Monajjemi^{2,*}

¹Department of Chemistry, Science and Research Branch, Islamic Azad University, Tehran, Iran

²Department of Chemical Engineering, Central Tehran Branch, Islamic Azad University, Tehran, Iran

*corresponding author e-mail address: Maj.monajjemi@iauctb.ac.ir

ABSTRACT

An approach has been accomplished to a structurally simpler photo-switch machine of prontosil antibacterial drug molecule with gamma cyclodextrin as rot-axon machine. In this system, upon to UV light the stable Trans structure is changed into the unstable of Cis configuration thermodynamically, while the opposite reaction can be operated with visible light. By this work, sulfamidochrysoidine (prontosil) with gamma cyclodextrin (γ CD) are simulated as an axle and a wheel respectively, while the boron nitride sheet (BNS) is used as a stopper. Prontosil into γ CD and combination with BNS can be used such a non-covalent system for photo-isomer-controlled machine. It has been exhibited a new system of molecular motor which works like a hinge motion, and has introduced as light-driven molecular hinges. The γ CD ring in the system can be reversibly switched through irradiation of wide range of UV and visible lights. This system can be applied for drug delivery of those antibiotics which cannot be used through straight injection.

Keywords: Rotaxane, Molecular Motor, h-BN, Switchable sensor, prontosil antibacterial

1. INTRODUCTION

A large diversity of molecular motors such as catenanes and rotaxanes has been synthesized by researchers [1-3]. Molecular machines are able to rotate in one direction based on temperature, pressure, pH, light and chemical reaction properties. Recently, several molecular motors are subject to Nano biological activities in viewpoint of energies, cyclic process, types of motion and finally the ways of monitoring as an operating system. These systems are categorized and works as the molecular shuttle, molecular propeller, molecular tweezers and molecular switches. A molecular switch works as a system which can reversibly change among a few stable states (mostly two states) which might change and shift in terms of pH, UV-visible photons, increase (or decrease) of temperature, electrical currents and the presence of a ligand.

Recently, artificial molecular machines and motors are designed based on rotaxanes which its name derives from the "rota" (a Latin word) and "axis" for wheel and axle¹, respectively. Rotaxanes are generally compounded of a molecule (axle-like) surrounded¹ by a macro molecular-ring (rota) and interrupted by a bulky group or a flat sheet as a stopper to prevent disassembling [2]. In this work, prontosil antibacterial as an Azo-benzene derived molecules with gamma cyclodextrin (γ CD) are simulated as an axle and a wheel respectively, while the h-BN sheet is used as a stopper (Fig.1). Prontosil molecule onto γ CD can be used such a complex system for photo-isomer- controlled machine [3]. So, a rational combination of h-BN and rotaxanes might present a new research way, given this fact which the presentation of rotaxanes onto h-BN sheets has not been accomplished previously. In this study, it has been reported a construction of photo-switchable-gamma-CD based on h-BN sheet. For achieving photo-switched⁴ in this machine, the system has been designed with two stopper-

sides including h-BN and dumb-bell-shaped components of SO_2NH_2 part of prontosil (Figs.1&2).

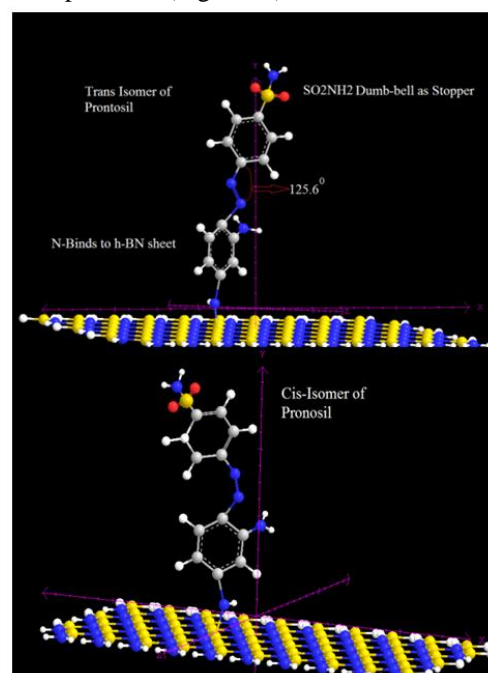


Figure 1. Optimized of the Molecular Motor including Cis & Trans isomers of prontosil.

The γ CD, which has hydrophobic cavities, serves as a host for forming an exclusive system with the prontosil molecule (as axle) including SO_2NH_2 segment that acts as a stopper in the end of one side. The system was then attached onto the surface of h-BN sheet via a Nitrogen atom (another part of prontosil molecule) and thus, h-BN acts as the second stopper on the other side of the machine. The γ CD in the system over the h-BN surface can move back and forth along the prontosil molecule axes

between the dumbbell components driven by cis-trans isomerization of the N=N part of prontosil molecule upon alternating irradiation⁴ with UV-visible light.

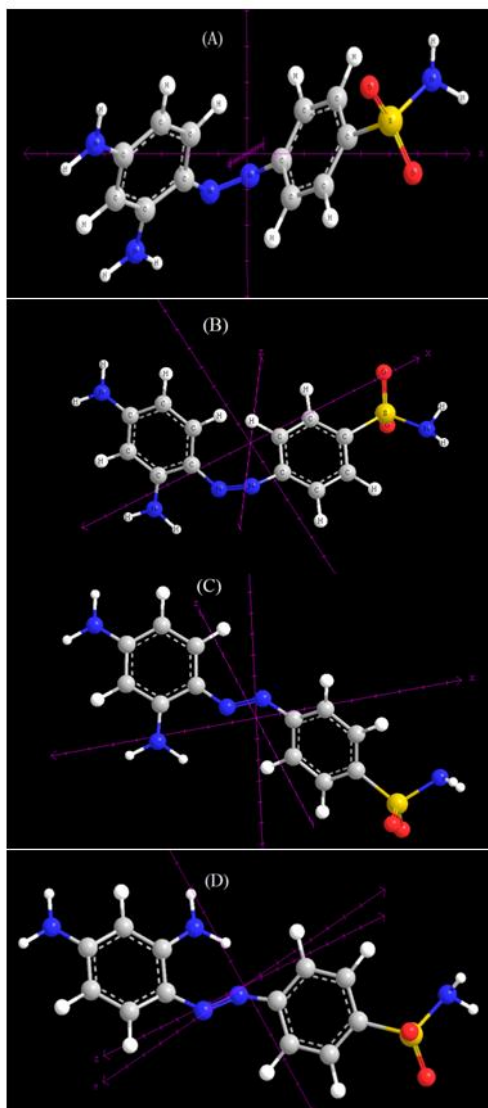


Figure 2. Various Dihedral conformational of Prontosil in several torsions degree of CNNC dihedrals (A=45°,B=180°,C=-45° and D=-180°).

2. EXPERIMENTAL SECTION

Computational details.

Each part of the machine including 3 sections of h-BN, γ CD and Prontosil has been optimized using abinitio with DFT calculations individually (Fig.3).

The whole of the h-BN sheet including γ CD and Prontosil axis has been calculated with QM/MM methods and the systems are accomplished with semi empirical methods.

In this work, differences of force fields are debated through comparing density and energies with OPLS and AMBER force fields. In addition, a Hyper-Chem professional release 7.01 program has been applied for some additional keywords such as PM3MM, PM6 (pseudo=lan12).

The final parameterization of Cis-trans isomerization of prontosil molecule was computed using SCF calculations in order to find

Cis-trans isomerization of Azo-benzene.

Cis-trans isomerization of Azo-benzene has been used for many functional [5] molecules with applications in photonics for several chemical systems.

These two isomers are able to switch with especial light wavelengths of ultraviolet regions, that corresponds to the different energies gap of the $\pi \rightarrow \pi^*$ transitions, for trans-to-Cis structures. In blue light region the $n \rightarrow \pi^*$ transition will occur for Cis-to-trans isomerization. Generally, the *Cis* isomer is less stable than the *Trans*. Although in our system, the *Trans* isomer is stable by approximately 25 kcal/mol than the *Cis*, the barrier energies of this isomerization (in the ground states) are much more than these values. In this study, we exhibited a new system of the molecular motor which works like a hinge motion, and has introduced as light-driven molecular hinges [6]. The characteristic [7] formation of a hinge-like molecule includes two planes which are attached to their edge sides through an axel; the motion of the hinge causes a conversion between closed and open states. We have exhibited that the UV-visible lights of our machine for the “prontosil - γ CD-h-BN” systems has a strong absorption band at 318.7 nm, which is corresponded to the $\pi - \pi^*$ transition in the trans- prontosil unit and the absorption disappeared after irradiation with UVA light which indicates that the system is impressed by the trans-cis changing. It might be noted that benzene has three aromatic $\pi \rightarrow \pi^*$ transitions; two E-bands at 180 and 200 nm and one B-band at 255 nm.

Prontosil as an Azo-benzene derived molecule with Cis-trans isomerization is an antibacterial drug discovered in 1932⁸ at the Bayer Laboratories

in Germany which has a relatively broad effect against Gram-positive and is not active in vitro. The discovery and development of this first sulfo-namide drug opened a new era in medicine [9].

Prontosil that was the result of a few years of testing involving hundreds of compounds related to Azo-dyes, has been replaced by newer sulfonamide, including sulfathiazole and sulfamethoxazole, in medicine drugs.

the optimal starting geometries, as well as the difference energies for these conformational structures (Fig.2&3). The DFT with the van der Waals densities functional was investigated for modeling of exchange-correlation estimation. All optimization of h-BN layers were performed by GAMESS-US package [10]. The accurate calculations performed using m062x, m06-L, and m06 for Cis-trans conformations. The m062x, m06-L and m06-HF methods have a suitable correspondence in non-bonded calculations between two isomers [11].

For non-covalent interactions between γ CD and prontosil molecule, the ONIOM methods including 3 levels of high (H), medium (M) and low (L) calculations have been done. DFT methods were used for the high (H) layer and the semi empirical

method of pm6 and Pm3MM was used for the medium and low layers, respectively.

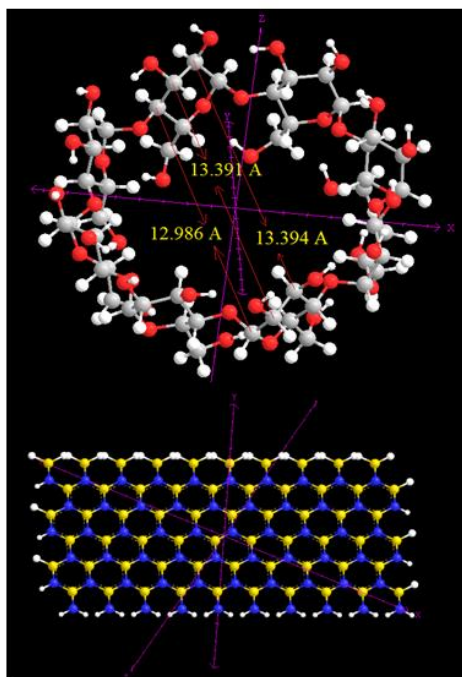


Figure 3. Optimized Gamma-cyclodextrin and optimized h-BN sheets.

The electrostatic potentials and charges transfer were also estimated using the Merz-Kollman-Singh, chelp, and chelp-G The

3. RESULTS SECTION

The light sensor rotaxanes arrays on the h-BN surfaces are able to increase the hybrid with new properties. In this work, h-BN is used as units from the boron nitride compounds and the covalent immobilization of the “UV& Visible-switchable-Rotaxane” which is a template-directed of a rational combination as the molecular motor (Fig.1). The Nitrogen covalent (Fig.1) instead of van der Waals interactions functionalization is beneficial to enhance the chemical stabilities of the Rotaxane-functionalized h-BN hybrid.

In this work, the prontosil axis was designed including SO_2NH_2 , as a stopper at one side and the N-h-BN's bridge at the other side. In this model, a wavelength of 318.7nm has resulted for the machine system (Table.1) which has a good agreement with the experimental result in the visible region. Hong Yan and coworkers [37] exhibited experimentally, that an absorption peak appears in the UV/vis spectrum, which corresponds to the 4-propargyloxybenzene unit and experimentally approves this theoretical work. In this study, only one stereoisomer in which the secondary side of the γCD rings faces the SO_2NH_2 stopper was demonstrated (Fig.1). In addition, it has been presented that the γCD ring in the Rotaxane can move back and forth between the prontosil-trans units upon trans-Cis isomerization (Fig.2 & table.1). Besides, the Trans-Cis and Cis-Trans isomers of the prontosil -system lead to two points whose results are confirmed experimentally [37]. Theoretically, the results exhibited two wavelengths around 318.7 nm and 231.3nm for two systems of Prontosil and F- Prontosil machines in UVA and UVB regions, respectively. As it can be seen in the Fig.1, the γCD ring in the

charge calculation method based on the molecular-electrostatic potentials (MESP) fitting is not well-fixed for treating larger systems whereas some of the innermost atom are located far away from the point at which the MESP is computed. The representative atomic charge for a molecule might be calculated as expectation values over several conformations. The interaction energies among various situations of Prontosil derived inside γCD were calculated in all items according to the equation:

$$\Delta E_i(\text{eV}) = \{E_{\text{sys}} - (E_{\text{h-BN}} + E_{\gamma\text{CD}} + E_{\text{prontosil}})\} + E_{\text{BSSE}} \quad (1)$$

Where the “ ΔE_i ” is the energy of the systems for various conformations of prontosil inside γCD . Several physical properties such as electron densities (Fig.6), values of orbital wave-functions, electron spin densities, , electron localization function (ELF), localized orbital locator (LOL defined by Becke & Tsirelson), total electrostatic potential (ESP), as well as the exchange-correlation densities, and the average local ionization energies (for two Cis-trans isomers) using the Multifunctional Wave-function analyzer have been also calculated for sulfur bridge[12] This molecular machine has been simulated based on a few fundamental properties such as ELF, LOL, non-bonded interactions and structures of stator and rotor motors which have been investigated in my previous works [13-36].

Rotaxane unit is primarily located at the Trans position, which is obviously far away from the surface of the h-BN and then γCD ring moves towards h-BN sheet position. In contrast of the previous position, the Trans-Cis transformation of the Prontosil system appears on upper wavelength, so the action of the γCD in forth and back wheel along the prontosil depends on two states of Rotaxane-functionalized h-BN sheet which is intrinsically useful for any light-sensors.

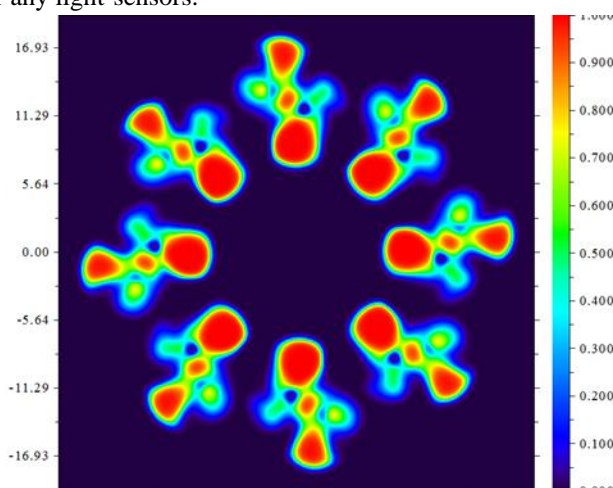


Figure 4. ELF for Cyclodextrin including 8 glucopyranoside units.

In extra calculations, the other groups (Br, F and Cl) were replaced instead of NH_2 in the second phenyl ring which interestingly the wavelength for the molecular machine shifts to down range in the

UVB (for F) and UVC(for Br and Cl) ultra-violets regions. In this work, our focus is partially based on the electron density, Hamiltonian kinetic energy $K(r)$, potential energy density $U(r)$, LOL, ELF and average local ionization energy of the sulfur atom when the Br, F and Cl groups have been replaced one by one in other side of prontosil system. The electron density (Fig.6) can be written as: $\rho(r) = \eta_i |\varphi_i(r)|^2 = \sum_i \eta_i |\sum_i C_{i,i} \chi_i(r)|^2$ (2)

Where the " η_i " indicates orbital's occupation number. As it can be seen in the table.2, the amount of those parameters are much more different for Nitrogen atom (attached to h-BN) in the system of Br-prontosil and Cl-prontosil compare to prontosil machine while the data for F-prontosil is similar to prontosil. One of the reasons is the different electronegativity of Chlorine and Bromine with Nitrogen which are larger than the Fluorine. Bader [38] has found that the big electron localization might have large values of Fermi-hole and Becke [39] and Edgecombe based on Bader's theory, suggested electron localization function (ELF) (equations 3-5) for the relation between spin pair probability with the Fermi hole.

$$ELF(r) = \frac{1}{1+[D(r)/D_0(r)]^2} \quad (3) \quad \text{where } D(r) = \frac{1}{2} \sum_i \eta_i |\nabla \varphi_i|^2 -$$

$$\frac{1}{8} \left[\frac{|\nabla \rho_\alpha|^2}{\rho_\alpha(r)} + \frac{|\nabla \rho_\beta|^2}{\rho_\beta(r)} \right] \quad (4) \quad \text{and}$$

$$D_0(r) = \frac{3}{10} (6\pi^2)^{\frac{2}{3}} [\rho_\alpha(r)^{\frac{5}{3}} + \rho_\beta(r)^{\frac{5}{3}}] \quad (5).$$

As it can be seen in the table .2, the ELF value for Nitrogen of h-BN (N^*) is larger than LOL in the systems of Cl-prontosil and Br-prontosil (both for cis and Trans) while this amount is shorter for prontosil and F-prontosil. ELF gives a relative localization and varied between the range of [0, 1]. A large amount of ELF up to 1 describes that electrons are completely localized and the large amounts indicate lone pair, a covalent bond or inner shells of the atoms.

In the table 2, the ELF in all systems is less than 0.5 which means the electron is not localized for the N-h-BN's bridge and makes flexibility for moving the Rotaxane back and forth between the Prontosil -axis and it's derivation units which were controlled by different wavelengths. This flexibility for Trans- prontosil and Trans-F- prontosil is more than Trans-Br- prontosil and Trans-Cl- prontosil machines due to the spatial barrier of Cl and Br compare to F and Displacement distances from Trans to cis of CD between two dumbbell components indicate those flexibilities (Table.3).

Savin *et al*[40]. have investigated the ELF in the viewpoint of kinetic energies, which indicated that $D(r)$ gives the excess kinetic energy densities caused by Pauli repulsion, while $D_0(r)$ can be thought-out as Thomas-Fermi kinetic energies. As it can be seen in Table1 & 2, the difference of Hamiltonian kinetic energies between Cis and Trans isomers for the F- prontosil is more than the Cl-prontosil and Br- prontosil machines , meanwhile potential energy density for Cis- prontosil and Cis-F- prontosil is positive while for the other systems is negative. It causes that the Cis-Br- prontosil and Cis-Cl- prontosil molecular motors cannot move to back and forth in the larger wavelengths (UVB & UVA) (Table 2) while they act in higher energies or shorter wavelengths (UVC) compare to Cis- prontosil and Cis-F- prontosil molecular motors.

LOL formalism is defined by Schmider and Becke²⁹.

$$LOL(r) = \frac{\tau(r)}{1+\tau(r)}, \quad \text{where } (r) = \frac{D_0(r)}{\frac{1}{2} \sum_i \eta_i |\nabla \varphi_i|^2} \quad (6)$$

LOL has a similar statement compared to ELF but the LOL (Fig.4) gives more definitive and explicit images than ELF.

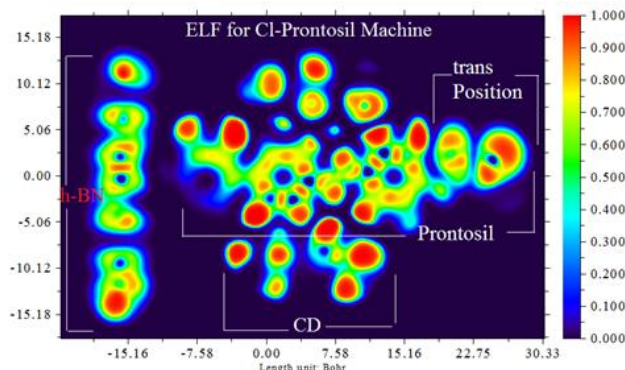


Figure 5. Color-Field Map of LOL for Trans, isomers of Prontosil which indicates the geometries, value of LOL and distances.

Based on eq.6, LOL can be demonstrated in kinetic energy path in contrast of ELF; small (large) LOL magnitude generally appears in border regions of localized orbital because the gradient of orbital wave-function is large (small) in this region. In table.2 the LOL is larger than the ELF for both Cis and Trans - prontosil and F- prontosil systems while it is smaller for Cl- prontosil and Br-prontosil which confirms the above interpretation. h-BN has been widely used for prediction of molecular recognition and intermolecular interaction of N-h-BN bonds. In other words, the total electrostatic potentials (ESP) measure the electrostatic interaction between Nitrogen point charges and the h-BN surface. The data of molecular electrostatic potential, average local ionization energies and electron densities are listed in the (table2, Fig.6).

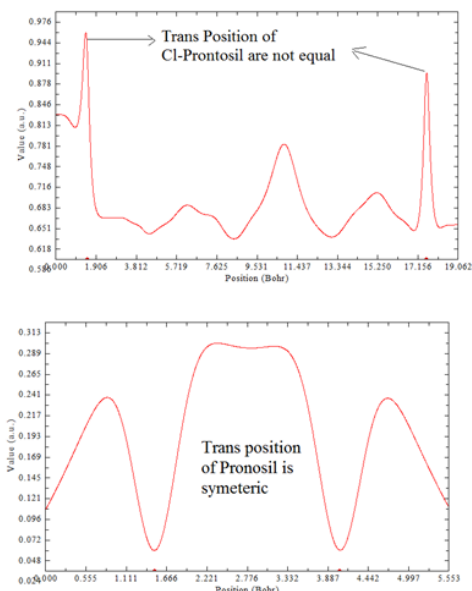


Figure 6. Electron densities for Cl-Prontosil-machines and Prontosil.

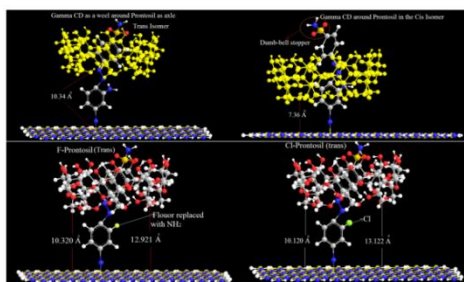
Table 1. The $\Delta E_{Trans-Cis}$ for Various machine as the Photo switchable Sensors.

| Axle systems | $\Delta E_{Trans\ to\ Cis}$ energy of Motor including (axle, wheel and Stopper) (Hartree) | $\Delta E_{Trans\ to\ Cis}$ For Switch (Kcal/mole) & Cm^{-1} respectively | The barrier energy For Switching (ev) | Wavelength (nm), Frequency (THZ) | Region of Photo switchable Sensor | Situation |
|---------------------------------|---|--|---------------------------------------|----------------------------------|-----------------------------------|---|
| F- Prontosil (Cis) to (Trans) | 0.03729 | 23.4, 8184.3 | 5.36 | 231.3, 1269 | Ultraviolet C (UVB) | Medium-wave, mostly absorbed by the ozone layer |
| Cl - Prontosil (Cis) to (Trans) | 0.041274 | 25.9, 9058.7 | 5.75 | 215.6, 1390 | Ultraviolet C (UVC) | Short Wave, <u>germicidal</u> , completely absorbed by the ozone layer and atmosphere |
| Br - Prontosil (Cis) to (Trans) | 0.039521 | 24.8, 8673.9 | 5.49 | 225.8, 1327 | Ultraviolet C (UVC) | Short Wave, <u>germicidal</u> , completely absorbed by the ozone layer and atmosphere |
| Prontosil Cis) to (Trans) | 0.033784 | 21.2, 7414.8 | 3.89 | 318.7, 940 | Ultraviolet A (UVA) | Long-wave, <u>black light</u> , not absorbed by the ozone layer |

Table 2. The Physical properties of Nitrogen-h-BN (N^*) bond in various system of Prontosil derivation in a same machine.

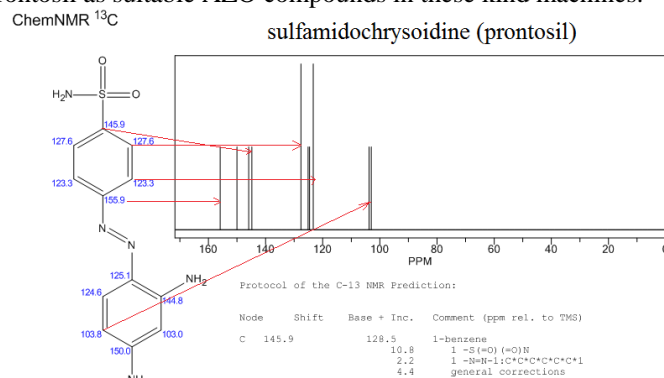
| N*-hBN in various Axle systems | Lumo/Homo Gap (kcal/mol) | | ELF & LOL | Local information entropy | U(r) & K(r) | $\sum LIE \& ESP$ |
|--------------------------------|--------------------------|------------------|--------------|---------------------------|----------------|-------------------|
| | α orbitals | β orbitals | | | | |
| Prontosil -cis | 3.28 | 1.02 | 0.157, 0.398 | 0.715 | 0.262, -0.130 | 0.769, -0.637 |
| Prontosil -trans | 4.11 | 10.22 | 0.112, 0.320 | 0.791 | -0.129, -0.429 | 0.805, -0.609 |
| Br- Prontosil -cis | 3.15 | 5.31 | 0.164, 0.127 | 0.721 | -0.198, -0.112 | 0.733, -0.701 |
| Br- Prontosil -trans | 0.30 | 4.12 | 0.304, 0.174 | 0.864 | -0.186, -0.129 | 0.823, -0.650 |
| Cl- Prontosil -cis | 2.15 | 1.03 | 0.213, 0.145 | 0.720 | -0.133, -0.119 | 0.706, -0.662 |
| Cl- Prontosil -trans | 2.613 | 2.10 | 0.308, 0.175 | 0.864 | -0.174, -0.120 | 0.799, -0.663 |
| F- Prontosil -cis | 3.28 | 1.03 | 0.187, 0.439 | 0.733 | 0.242, -0.127 | 0.779, -0.655 |
| F- Prontosil -trans | 4.27 | 11.51 | 0.122, 0.305 | 0.843 | -0.143, -0.55 | 0.835, -0.608 |

All data are approximately equal and negative (Table2) and a negative value implies that the current position is dominated by nuclear charges (not electronic charges), so they are independent of halogens radiuses and depends only to h-BN surface properties. The distances between h-BN sheet and αCD for Functional groups- prontosil along the N- prontosil axis (Fig.7 & Table3) are not equal in the right and left sides of the machines which indicate that the axis has a deviation from the h-BN surface.

**Figure 7.** The distances between h-BN and γCD for Prontosil (cis & Trans), Cl-Prontosil and F-Prontosil machines along the axis.

The changing of these deviations caused the γCD in the machine over the h-BN surface easily moved back and forth along the prontosil axle. As it can be seen in the table 3, the changing of these distances in the left side (in contrast the right side) is approximately equal which indicates that this movement is monotonous in one direction. The carbon NMR shielding of

Prontosil (Fig.8) has been calculated for the verification of using Prontosil as suitable AZO compounds in these kind machines.

**Figure 8.** The carbon NMR shielding of Prontosil.**Table 3.** Displacement distances from Trans to cis of CD between two dumbbell components

| Displacements | Right side (angstrom) | Left side (angstrom) |
|------------------------|-----------------------|----------------------|
| Prontosil -machine | 3.61 | 3.71 |
| F- Prontosil -machine | 3.65 | 3.75 |
| Cl- Prontosil -machine | 3.50 | 3.70 |
| Br- Prontosil -machine | 3.45 | 3.69 |

4. CONCLUSIONS

We have successfully modeled a system to introduce light-sensor of γCD -based rotaxanes over the h-BN sheet. The γCD

ring in the system can be reversibly switched through irradiation of wide range of UV (UVC, UVB and UVA) lights. Through

changing the functional groups in one side (with halogens in this work) and fixing it in another side of dumb-bell ring, various systems in a wide range of UV sensors can be simulated to predict a model for any further experiments of designing molecular machines. Through changing the functional groups in one side and

fixing it in another side of dumb-bell ring, various systems in wide range of UV sensors can be simulated to predict a model for any further experiments of designing molecular machines. These kind machines are suitable for drug delivery in nano technology subjects.

5. REFERENCES

- [1] Balzani V., Credi A., Venturi M. A., Journey into the Nano World, Wiley-VCH, Weinheim, Published Online: **2004**.
- [2] Dietrich-Buchecker C., Rapenne G., Sauvage J.P., Molecular Knots - From Early Attempts to High-Yield Template Syntheses, Wiley on line library, Chapter 6, **2007**.
- [3] Yan H., Teh C., Sreejith S., Zhu L., Kwok A., Fang W., Ma X., Nguyen K. T., Korzh V., Zhao Y. L., photothermalcontrolled drug delivery in vivo, *Angew. Chem. Int. Ed.* 51, 8373–8377, **2012**.
- [4] Ashton P.R., Ballardini R., Balzani V., Credi A., Dress K.R., Ishow E., Kleverlaan C.J., Kocian O., Preece J.A., Spencer N., Stoddart J.F., Venturi M., Wenger S. A Photochemically Driven Molecular-Level Abacus, *Chem. Eur. J.* 6, 3558. **2000**.
- [5] Shinkai S., Ogawa T., Nakaji T., Kusano Y., Manabe O, Photocontrolled extraction ability of azobenzene-bridged azacrown ether, *Tetrahedron Lett*, 1979, 47, 4569 – 4572, **1979**.
- [6] Hirst C.S., Hamilton A.D., Molecular recognition: Cyclobutane thymine diners as rigid two-site receptors, *Tetrahedron Letters*, 31, 17, 2401-2404, **1990**.
- [7] Shinkai S., He G.-X., Matsuda T., Hamilton A. D., Rosenzweig H. S., Specific inhibition of flavin catalyses by a "molecular hinge", *Tetrahedron Lett.*, 30, 5895 – 5898, **1989**.
- [8] Oxford Handbook of Infectious Diseases and Microbiology, OUP, oxford, 56, ISBN 9780191039621. **2009**.
- [9] Hager, Thomas: *The Demon under the Microscope: From Battlefield Hospitals to Nazi Labs, One Doctor's Heroic Search for the World's First Miracle Drug*. Harmony Books, ISBN 1-4000-8214-5 , **2006**.
- [10] Schmidt M.W., Baldrige K.K., Boatz J A., Elbert S.T., Gordon M.S., Jensen J.H., Koseki S., Matsunaga N., Nguyen K.A., Gamess Package of abinitio, *J Comput Chem*, 14, 11,1347–1363, **2004**.
- [11] Zhao Y., Truhlar D.G., The M06 suite of density functionals for main group thermochemistry, thermochemical kinetics, noncovalent interactions, excited states, and transition elements: two new functionals and systematic testing of four M06-class functionals and 12 other functionals, *Theor Chem Account*, 120, 215–241, **2008**.
- [12] Lu T., Chen F., Multiwfn: A Multifunctional Wavefunction Analyzer, *J. Comp. Chem.*, 33, 580-592, **2012**.
- [13] Monajjemi M., Mohammadian N.T., S-NICS an Aromaticity Criterion for Nano Molecules, *J. Comput. Theor. Nanosci*, 12, 4895-4914, **2015**.
- [14] Monajjemi M., Lee V.S., Khaleghian M., Honarparvar B., Mollaamin F., Theoretical Description of Electromagnetic Nonbonded Interactions of Radical, Cationic, and Anionic NH₂BHNH₂ Inside of the B18N18 Nanoring, *J. Phys. Chem C*, 114, 15315, **2010**.
- [15] Monajjemi M., Boggs J.E., A New Generation of BnNn Rings as a Supplement to Boron Nitride Tubes and Cages, *J. Phys. Chem. A*, 117, 1670 –1684, **2013**.
- [16] Monajjemi M., Non bonded interaction between BnNn (stator) and BN B (rotor) systems: A quantum rotation in IR region, *Chemical Physics*, 425, 29-45, **2013**.
- [17] Monajjemi M., Wayne Jr Robert., Boggs J.E., NMR contour maps as a new parameter of carboxyl's OH groups in amino acids recognition: A reason of tRNA–amino acid conjugation, *Chemical Physics*, 433, 1-11, **2014**.
- [18] Monajjemi M., Quantum investigation of non-bonded interaction between the B15N15 ring and BH₂NBH₂ (radical, cation, and anion) systems: a nano molecular motor, *Struct Chem*, 23, 551–580, **2012**.
- [19] Monajjemi M., Non-covalent attraction of B₂N (2, 0) and repulsion of B₂N (+) in the BnNn ring: a quantum rotatory due to an external field, *Theor Chem Acc*, 1668-9, **2015**.
- [20] Monajjemi M., Metal-doped graphene layers composed with boron nitride–graphene as an insulator: a nano-capacitor, *Journal of Molecular Modeling*, 20, 2507, **2014**.
- [21] Monajjemi M., Najafpour J., Charge density discrepancy between NBO and QTAIM in single-wall armchair carbon nanotubes, *Fullerenes Nanotubes and Carbon Nanostructures*, 22, 6, 575-594, **2014**
- [22] Mollaamin F., Monajjemi M., DFT outlook of solvent effect on function of nano bioorganic drugs, *Physics and Chemistry of Liquids*, 50, 5, 596-604, **2012**
- [23] Mahdavian L., Monajjemi M., Mangkorntong N., *Fullerenes Nanotubes and Carbon Nanostructures*, 17, 5, 484-495, **2009**
- [24] Monajjemi M., Cell membrane causes the lipid bilayers to behave as variable capacitors: A resonance with self-induction of helical proteins, *Biophysical Chemistry*, 207, 114 –127, **2015**.
- [25] Monajjemi M., Mahdavian L., Mollaamin F., Interaction of Na, Mg, Al, Si with carbon nanotube (CNT): NMR and IR study *Russian Journal of Inorganic Chemistry*, 54, 9, 1465-1473, **2009**.
- [26] Monajjemi M., Liquid-phase exfoliation (LPE) of graphite towards graphene: An ab initio study, *Journal of Molecular Liquids*, 230, 461 –472, **2017**.
- [27] Monajjemi M., Study of CD⁵⁺ Ions and Deuterated Variants (CH_xD(5-x)⁺): An Artefactual Rotation, *Russian Journal of Physical Chemistry a*, 92, 11, 2215-2226, **2018**
- [28] Alemi-Tameh F., Safaei-Ghomi J., Mahmoudi-Hashemi M., Monajjemi M., Amino Functionalized Nano Fe₃O₄@SiO₂ as a Magnetically Green Catalyst for the One-Pot Synthesis of Spirooxindoles Under Mild Conditions, *Polycyclic Aromatic* 38, 3, 199-212, **2018**
- [29] Elsagh A., Zare K., Monajjemi M., Calculation of the magnetic resonance isotropy tensors of the nucleus of POPC phospholipid bilayers in a cell membrane, *Ukrainian Journal of Ecology*, 8, 1, 165-173, **2018**
- [30] Zakeri M., Monajjemi M., Effective molecules of some natural product as antidepressant and antihistamine drugs: A NMR study, *Ukrainian Journal of Ecology*, 8, 2, 255-262, **2018**
- [31] Bagheri S., Aghaei H., Monajjemi M., Novel Au-Fe₃O₄ NPs Loaded on Activated Carbon as a Green and High Efficient Adsorbent for Removal of Dyes from Aqueous Solutions: Application of Ultrasound Wave and Optimization, *Eurasian Journal of Analytical Chemistry*, 13, 3, **2018**
- [32] Moosavi M. S., Monajjemi M., Zare K., A Nano Catalyst of Cofe(2)o(4)@ B18N18 as A Novel Material, *Oriental Journal of Chemistry*, 33, 4, 1648, **2017**
- [33] Monajjemi M., GRAPHENE/(h-BN)(n)/X-DOPED GRAPHENE AS ANODE MATERIAL IN LITHIUM ION BATTERIES, *Macedonian Journal of Chemistry and Chemical Engineering*, 36, 1, 101-118, **2017**
- [34] Farhami N., Monajjemi M., Zare K., Non Bonded Interactions in cylindrical capacitor of (m, n) @ (m', n') @ (m'', n'') Three Walled Nano Carbon Nanotubes, *Oriental Journal of Chemistry*, 33, 6, 3024-3030, **2017**
- [35] Madani M. S., Monajjemi M., Aghaei H., The Double Wall Boron Nitride Nanotube: Nano-Cylindrical Capacitor, *Oriental Journal of Chemistry*, 33, 3, 1213-1222, **2017**
- [36] Shahriari S., Monajjemi M., Zare K., Increasing the efficiency of some antibiotics on penetrating bacteria cell membrane, *Ukrainian Journal of Ecology*, 8, 1, 671-679, **2018**
- [37] Yan H., Zhu L., Li X., Kwok A., Ågren H., Zhao Y., Photothermal-responsive [2] rotaxanes, *RSC Adv*, 3, 2341-2350, **2013**.
- [38] Bader R.F.W., Atoms in Molecule: A quantum Theory, *Oxford Univ. press, Oxford*, **1990**.
- [39] Becke A.D., Edgecombe A., simple measure of electron localization in atomic and molecular systems, *The Journal of Chemical Physics*, 92, 9, 5397-5403, **1990**.
- [40] Savin A., Nesper R., Wengert S., Fassler T., ELF: The Electron Localization Function, *Angew. Chem. Int. Ed. Engl.*, 36, 17, 1808-1832, **1997**.